

**Electronic Supplemental Information (ESI)**  
**for**  
**Molten-droplet-driven growth of MoS<sub>2</sub> flakes with controllable morphology**  
**transition for hydrogen evolution reaction**

Shuai Yang,<sup>‡a</sup> Jing Wu,<sup>‡a</sup> Chao Wang,<sup>a</sup> Hong Yan,<sup>a</sup> Luoqiao Han,<sup>a</sup> Jianmin Feng,<sup>a</sup> Bo Zhang,<sup>a</sup> Dejun Li,<sup>a</sup> Gui Yu<sup>\*b, c</sup> and Birong Luo<sup>\*a</sup>

<sup>a</sup>College of Physics and Materials Science, Tianjin Normal University, Tianjin 300387, P. R. China.

<sup>b</sup>Beijing National Laboratory for Molecular Sciences, Institute of Chemistry, Chinese Academy of Sciences, Beijing 100190, P. R. China.

<sup>c</sup>School of Chemical Sciences, University of Chinese Academy of Sciences, Beijing 100049, P. R. China.

## 1 Experiment parameters

Table. S1 The experiment parameters of the MDD growth of MoS<sub>2</sub> on Si/SiO<sub>2</sub> surfaces by chemical vapor deposition.

C <sub>NaOH</sub> (mM)	M <sub>MoO<sub>3</sub></sub> (mg)	Heating up time (min)	Growth time (min)	growth temperature (°C)	Gas flow (sccm)
200	80	20	10	800	200
200	80	20	10	820	200
200	80	20	10	840	200
200	80	20	10	860	200
200	80	20	10	880	200

## 2 Supplementary Figures

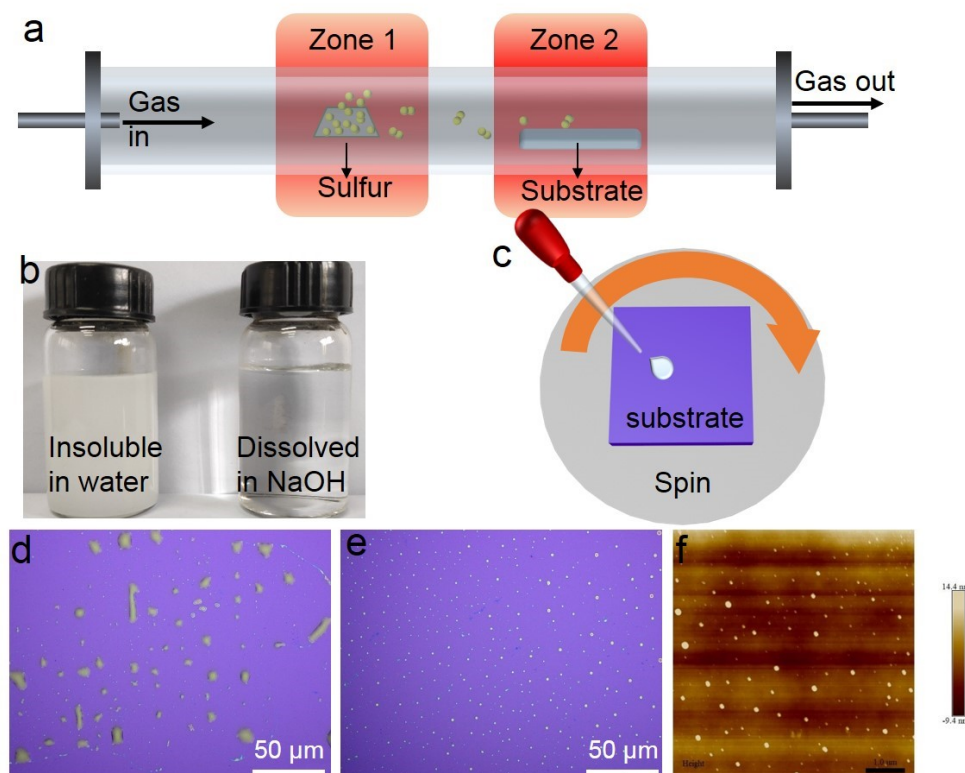


**Fig. S1** (a) Schematic diagram of the dual-temperature CVD system for synthesizing MoS<sub>2</sub> domains. (b) Optical images of MoO<sub>3</sub> powder dissolved in NaOH solutions, showing the solubility of MoO<sub>3</sub> in NaOH. (c) Schematic diagram of liquid-precursor uniformly spin-coated on SiO<sub>2</sub>/Si for the growth. (d) Optical image of liquid precursor spin-coated on SiO<sub>2</sub>/Si substrate. (e) Optical and (f) AFM topography image of the liquid precursor spin-coated on the SiO<sub>2</sub>/Si substrate after drying.

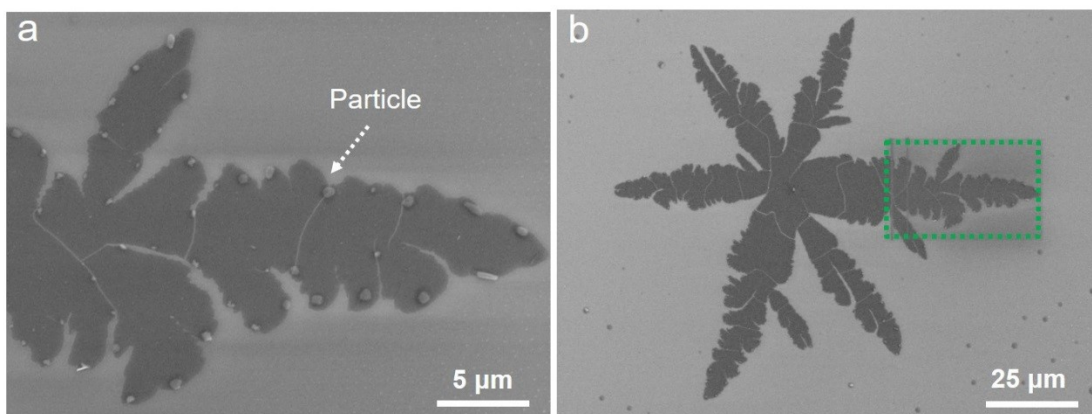


**Fig. S2** (a) High-magnified SEM image of the spike taken from the green frame in (b) low-magnification SEM of a MDD-grown MoS<sub>2</sub> flake at growth temperature of 880°C, showing that the edges of the MoS<sub>2</sub> flakes are uniformly surrounded by solidified droplets.

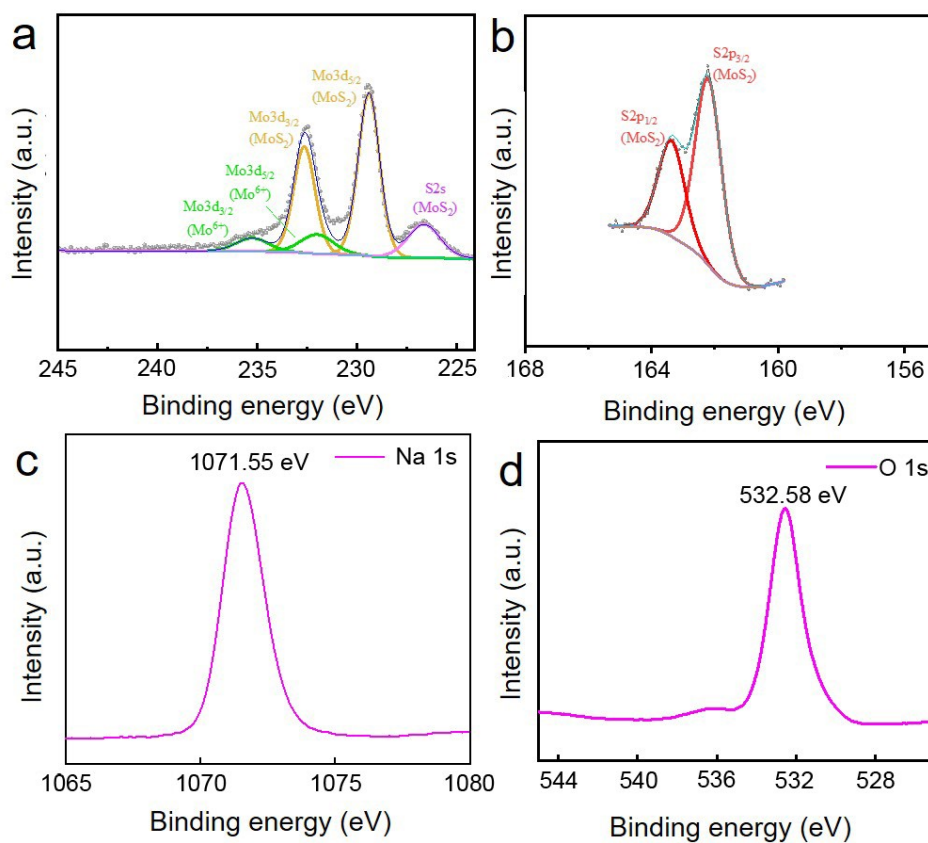


**Fig. S3** XPS spectra of the MDD-grown MoS<sub>2</sub> flakes, showing (a) Mo 3d, (b) S 2p, (c) Na 1s, and (d) O 1s XPS peak.

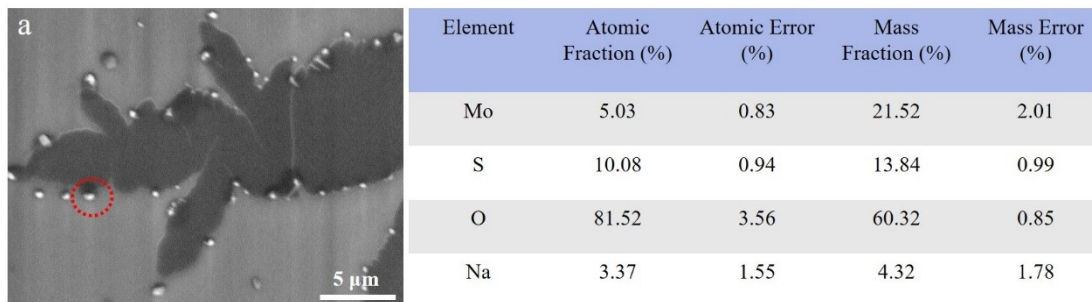


**Fig. S4** (a) High-magnification SEM of a MDD-grown MoS<sub>2</sub> edge at growth temperature of 880 °C, and (b) the corresponding EDS analysis for the particles denoted as the red circle in (a). Please note that here the irrelevant elements (Si and C) are not included for the EDS analysis.

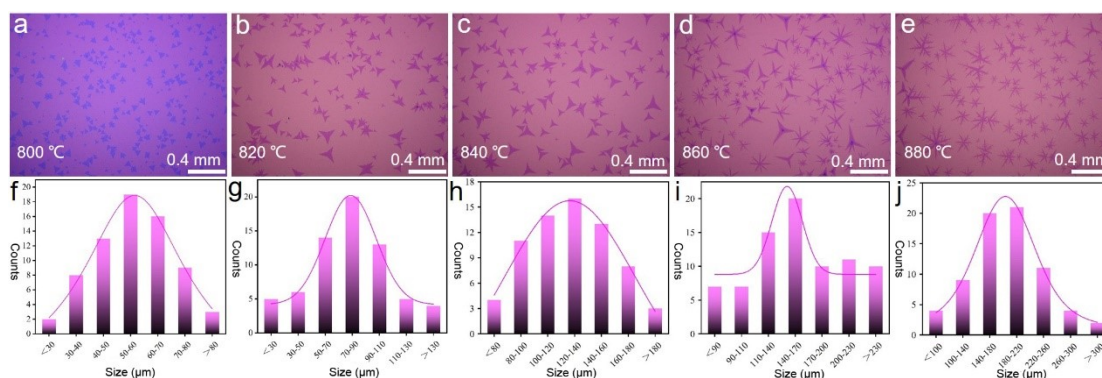


**Fig. S5** (a-e) Optical images of MDD-grown MoS<sub>2</sub> flakes at growth temperatures of (a) 800, (b) 820, (c) 840, (d) 860, and (e) 880 °C, respectively. (f-j) The corresponding lateral size statistics of MoS<sub>2</sub> flakes in (a-e).

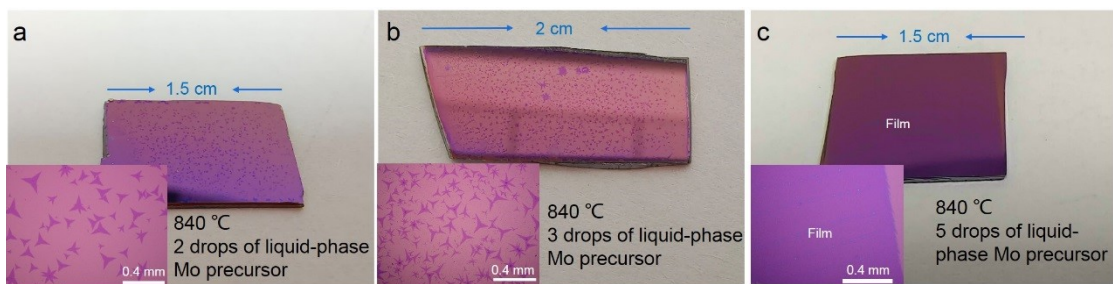


**Fig. S6** (a-c) Optical image of MoS<sub>2</sub> flakes on SiO<sub>2</sub>/Si substrate grown by MDD growth with different Mo precursor amount at fixed 840 °C and 10 min growth. The insets are randomly taken from the corresponding substrate.

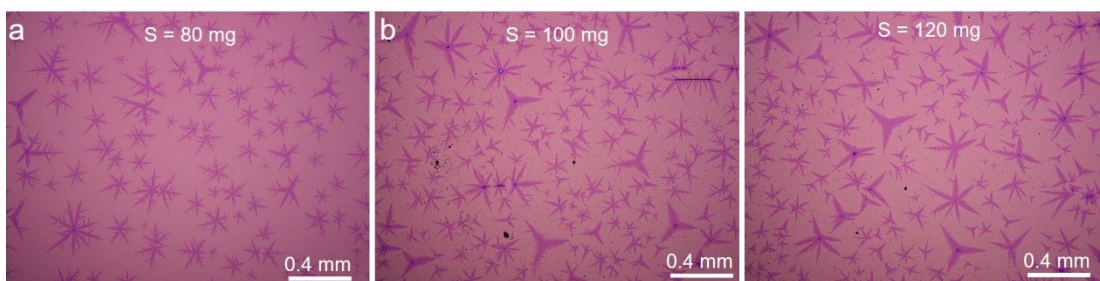


**Fig. S7** (a-c) Optical images of MoS<sub>2</sub> flakes on SiO<sub>2</sub>/Si substrate grown by MDD growth with different S precursor amount at fixed 880 °C and 10 min growth.

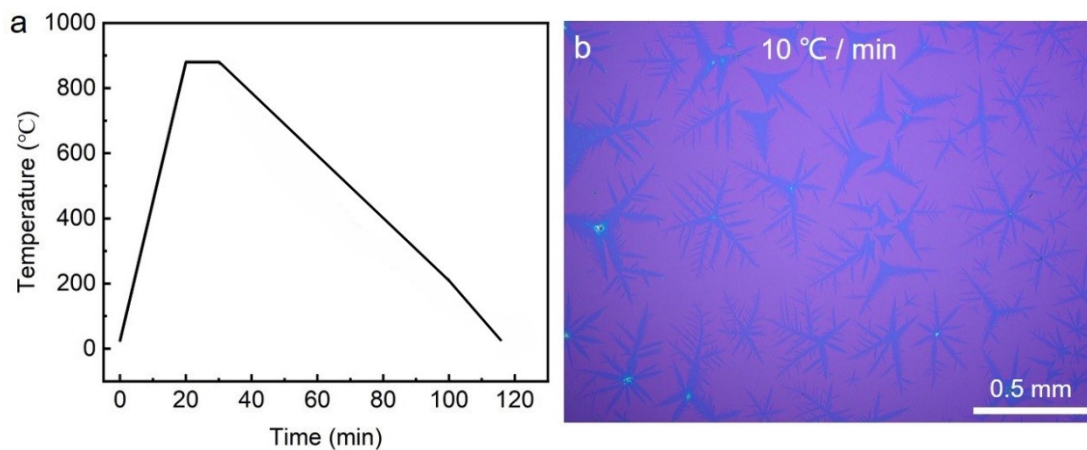


**Fig. S8** (a) The temperature curve with a slow cooling rate of 10 °C/min in the MDD growth process. (b) Optical images of MoS<sub>2</sub> crystals at a growth temperature of 880 °C and a cooling rate of 10 °C /min with otherwise identical conditions.

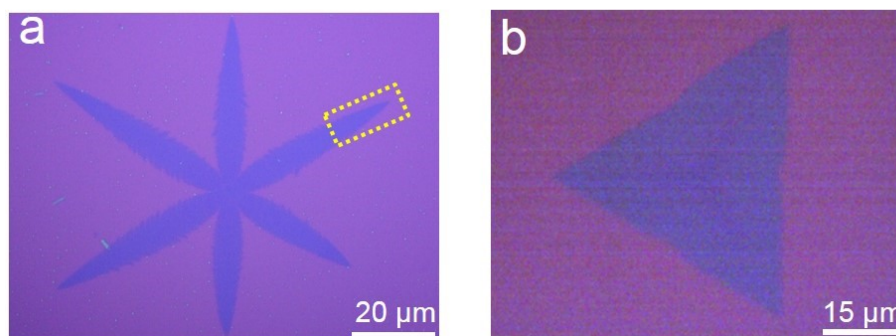


**Fig. S9** (a) Optical image of dendritic MDD-grown MoS<sub>2</sub> flake for the optical properties characterization. The inset yellow frame is the area for Raman and PL mapping measurements shown in Fig. 3c and e. (b) Optical image of triangular MDD-grown MoS<sub>2</sub> flake for the optical properties characterization.

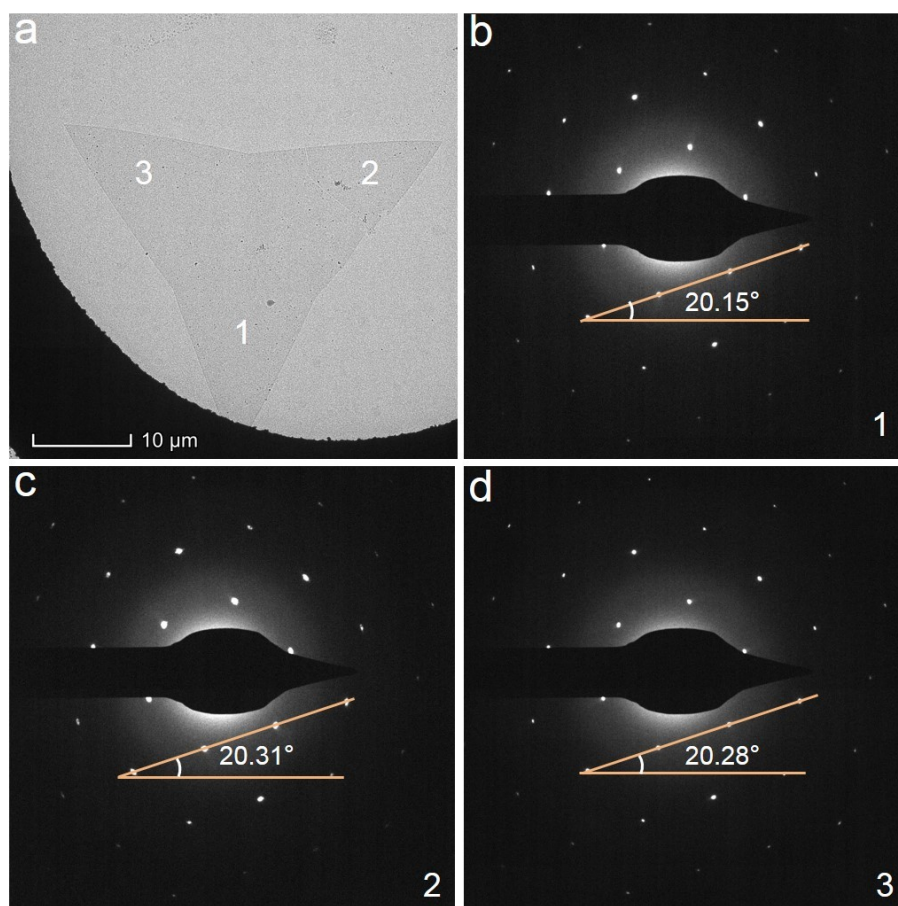


**Fig. S10** (a) TEM images of the triangle-shaped MoS<sub>2</sub> flake transferred on copper grid. (b-d) Selected area electron diffraction (SAED) patterns for selected regions at different locations marked as 1, 2, and 3 in (a).



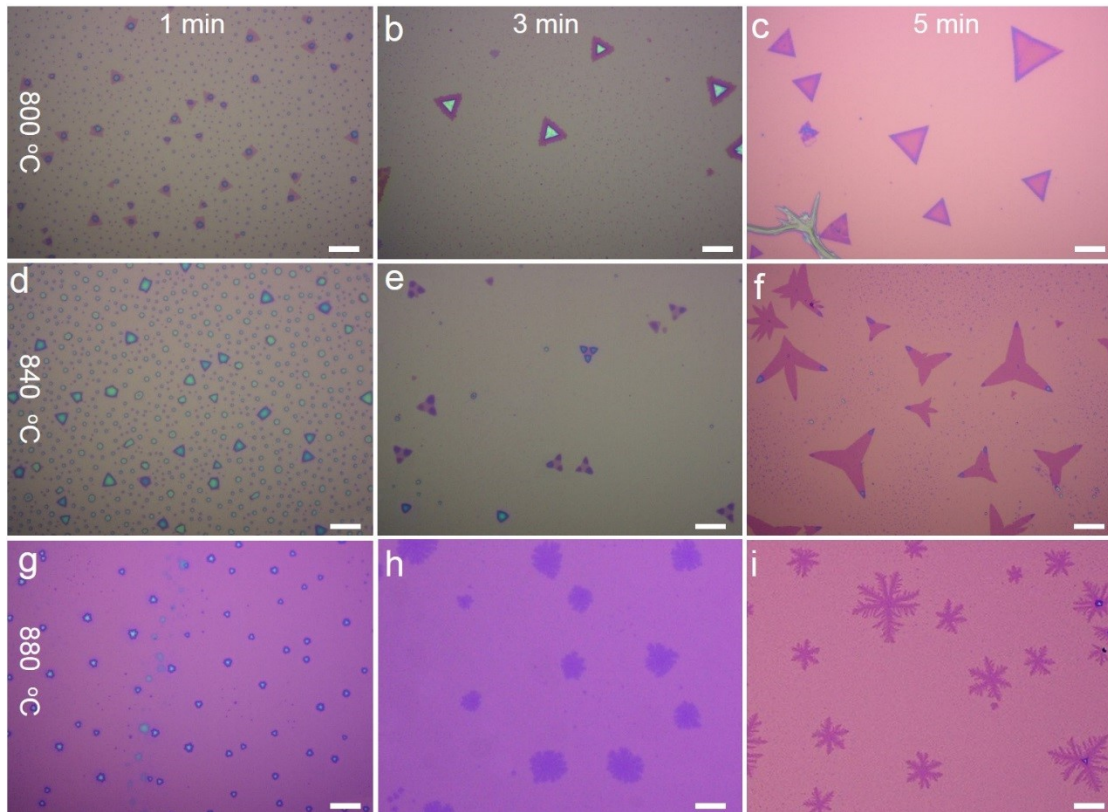


**Fig. S11** (a-c) Low-magnification optical images of MDD-grown MoS<sub>2</sub> flake on substrate for 1, 3, and 5 min growth at 800 °C. (d-f) Low-magnification optical images of MDD-grown MoS<sub>2</sub> flake on substrate for 1, 3, and 5 min growth at 840 °C. (g-i) Low-magnification optical images of MDD-grown MoS<sub>2</sub> flake on substrate for 1, 3, and 5 min growth at 880 °C. All the scale bar is 20 μm.

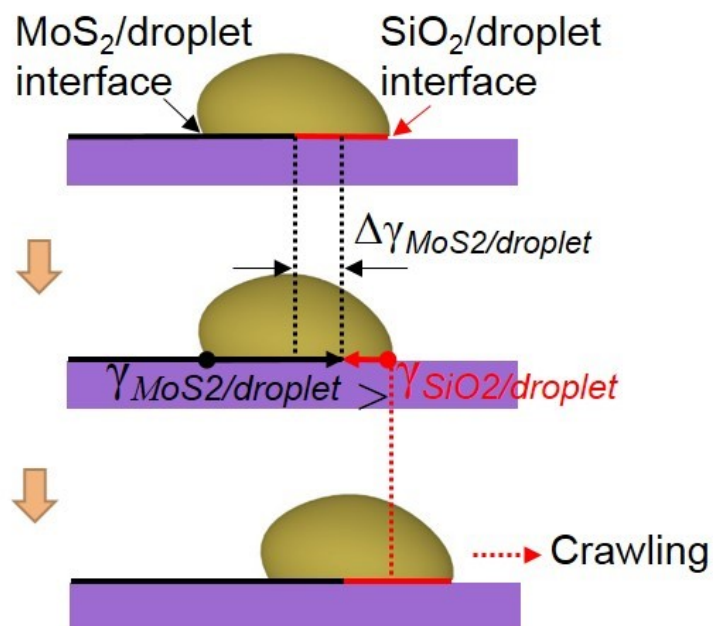


**Fig. S12** Schematic of driven molten droplet with crawling movement during the growth of MoS<sub>2</sub>.  $\gamma_{\text{MoS}_2/\text{liquid}}$  and  $\gamma_{\text{SiO}_2/\text{liquid}}$  are the interface energies of solid MoS<sub>2</sub> and SiO<sub>2</sub>/liquid droplet, respectively.  $\Delta\gamma_{\text{MoS}_2/\text{liquid}}$  is the interface energy of solid MoS<sub>2</sub>/liquid droplet of accretion growth of MoS<sub>2</sub>.

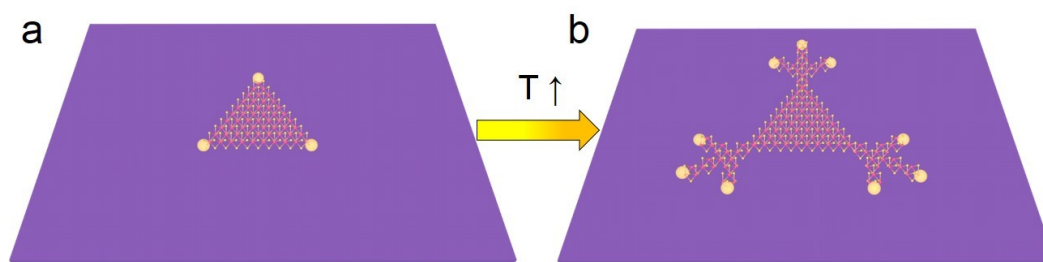


**Fig. S13** (a, b) Schematic diagram of a MoS<sub>2</sub> flake grown at an initial growth temperature of 840°C (a) for 4 minutes and then rapidly ramped up to 880°C (b) for 5 minutes.

## Supplementary Note

**Calculation of the fractal dimension of MoS<sub>2</sub> flakes.** In order to quantify the complexity of the MoS<sub>2</sub> morphology under different experimental conditions, we used box-counting to evaluate it. In this method, the image is filled with boxes of a certain number of pixels, and the number of pixels in the boxes is calculated by the size of the Fig.. The number of boxes for each filled Fig. is analyzed after enlarging and shrinking the Fig. by a certain scale. Therefore, we use the following method to calculate:

$$\text{Log}(N) = -D\text{Log}(s) + \text{Log}(C)$$

where N is the number of boxes, s is the scale of the graph, and D is the fractal dimension. The higher the fractal dimension, the more complex the graph structure.